

Electromechanical Impedance Based Structural Health Monitoring of Steel Frame Structure Using Surface Bonded PZT Sensors

Siddharth Mahadeo Tayade¹, Avinash D. Jakate², Dr.Suchita K. Hirde³

¹Student, M.Tech(Structural Engineering), Government College of Engineering, Amravati, Maharashtra, India

²Lecturer in Civil Engineering Department, Government Polytechnic, Amravati, Maharashtra, India

³Professor & Head, Applied Mechanics Department, Government College of Engineering, Amravati, Maharashtra, India

Abstract - Structural Health Monitoring (SHM) has become an important research area in civil engineering for ensuring safety and durability of engineering structures. Among various SHM techniques, the Electromechanical Impedance (EMI) method using Piezoelectric (PZT) sensors is highly sensitive for detecting localized structural damage. The present study experimentally investigates the effectiveness of the EMI technique for damage detection in a steel frame structure using 36 surface bonded PZT sensors. Experimental impedance signatures were acquired using an LCR meter under healthy condition, mass addition condition, and partial bolt removal condition. The acquired data were processed using MATLAB for impedance analysis, conductance analysis, RMSD analysis, AMSD analysis, correlation coefficient analysis, peak frequency shift analysis, and heatmap-based damage localization. The results indicated significant impedance variation under damaged conditions, particularly in the partial bolt removal case due to stiffness degradation. Sensor 3 exhibited the maximum RMSD value, confirming high local damage sensitivity. The study validates that the EMI technique provides an accurate, reliable, and economical approach for real-time structural damage detection and localization.

Keywords - Structural Health Monitoring, Electromechanical Impedance, PZT Sensor, RMSD, Damage Detection, Steel Frame Structure, EMI Technique.

1.INTRODUCTION

Structural deterioration due to aging, excessive loading, corrosion, fatigue, and connection loosening can significantly reduce the safety and service life of engineering structures. Conventional inspection techniques are often unable to identify localized structural damage at an early stage. Therefore, development of reliable Structural Health Monitoring (SHM) systems has become essential for modern infrastructure.

The Electromechanical Impedance (EMI) technique using Piezoelectric (PZT) sensors has emerged as a promising smart sensing method for real-time structural monitoring. The EMI method is based on the electromechanical coupling behavior of PZT materials, where structural damage produces variation in impedance signatures due to changes in local stiffness and dynamic characteristics [1].

Several researchers have successfully applied EMI techniques for damage detection in steel and concrete structures [2–5]. However, limited studies are available on multi-sensor impedance-based monitoring of steel frame structures under multiple damage conditions. Therefore, the present investigation focuses on experimental validation of EMI-based SHM using 36 bonded PZT sensors installed on a steel frame structure.

The impedance signatures obtained from an LCR meter were processed using MATLAB for graphical and statistical analysis. The effectiveness of the proposed methodology was

validated using RMSD, AMSD, correlation coefficient, peak frequency shift, and heatmap localization techniques.

2.OBJECTIVES

The objectives of the present investigation are:

1. To experimentally investigate EMI-based SHM for steel frame structures.
2. To study impedance signature variation under healthy and damaged conditions.
3. To evaluate the effect of mass addition and partial bolt removal on structural response.
4. To perform MATLAB-based impedance signal processing and statistical analysis.
5. To localize structural damage using RMSD-based heatmap analysis.
6. To validate the effectiveness of PZT sensors for real-time structural monitoring.

3. EXPERIMENTAL METHODOLOGY

3.1 Experimental Steel Frame Structure

The experimental investigation was carried out on a laboratory-scale steel frame structure consisting of multiple beam-column connections. The structure was designed to simulate practical structural behavior under different damage scenarios.



Fig 1: Experimental Steel Frame Structure Used for EMI Analysis

3.2 PZT Sensor Installation

A total of 36 surface bonded PZT sensors were installed at different structural locations using adhesive bonding. The sensor arrangement was selected to monitor local structural response throughout the frame.

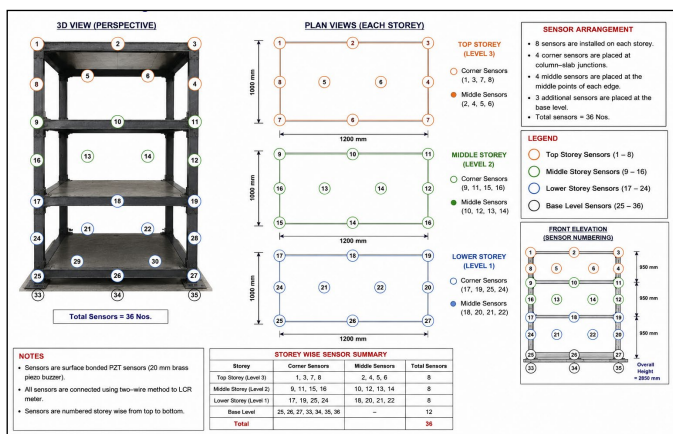


Fig 2: Arrangement of 36 Surface Bonded PZT Sensors on Steel Frame

3.3 Experimental Damage Conditions

Three structural conditions were considered during the experimental investigation:

1) Healthy Condition

The structure was maintained in undamaged condition to obtain baseline impedance signatures.

2) Mass Addition Condition

Additional mass was introduced at selected locations to study variation in resonance behavior.

3) Partial Bolt Removal Condition

Partial loosening/removal of bolts was introduced to simulate stiffness degradation.



Fig 3: Mass Addition Damage Condition



Fig 4: Partial Bolt Removal Damage Condition

3.4 Data Acquisition Using LCR Meter

The impedance signatures were obtained using an LCR meter over a selected frequency range. The experimentally acquired data were exported to Excel format and processed using MATLAB. The frequency range of 10 kHz–400 kHz was selected to maximize local electromechanical coupling sensitivity while minimizing dominance of global structural

vibration modes. Higher frequency excitation improves localized impedance sensitivity toward minor stiffness degradation and structural discontinuities.



Fig 5: Experimental Setup for EMI Data Acquisition Using LCR Meter

3.4 MATLAB Based Signal Processing

The acquired impedance signatures were processed using MATLAB for graphical and statistical analysis.

The following analyses were performed:

- Impedance analysis
- Conductance analysis
- RMSD analysis
- AMSD analysis
- Correlation coefficient analysis
- Peak frequency shift analysis
- Heatmap damage localization

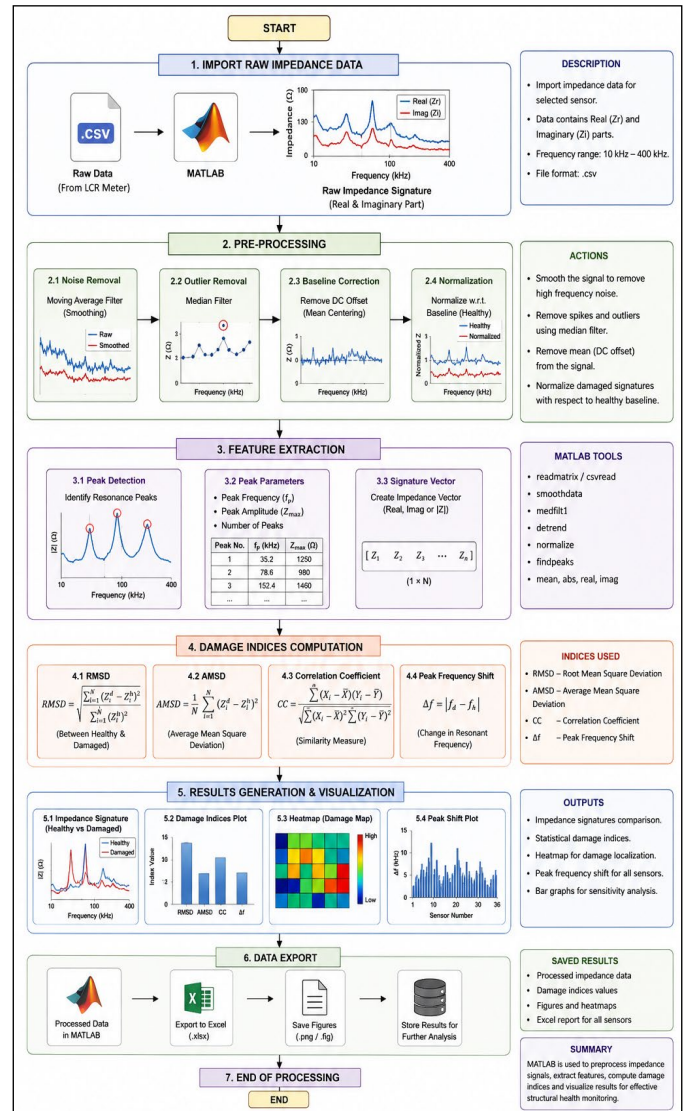


Fig 6: MATLAB Based Signal Processing Procedure

4. SIGNAL PROCESSING AND STATISTICAL ANALYSIS

4.1 RMSD Analysis

The Root Mean Square Deviation (RMSD) index was used to quantify the deviation between healthy and damaged impedance signatures.

$$RMSD = \sqrt{\frac{\sum_{i=1}^N (Z_i^d - Z_i^h)^2}{\sum_{i=1}^N (Z_i^h)^2}}$$

where:

Z_i^h = Healthy impedance signature

Z_i^d = Damaged impedance signature

N = Number of frequency points

Sample Calculation for Sensor 3

Healthy impedance values:

[52.4, 53.1, 54.2]

Damaged impedance values:

[58.6, 60.1, 61.4]

Difference:

$(58.6 - 52.4) = 6.2$

$(60.1 - 53.1) = 7.0$

$(61.4 - 54.2) = 7.2$

Squared difference:

$6.2^2 = 38.44$

$7.0^2 = 49.00$

$7.2^2 = 51.84$

$$RMSD = \sqrt{\frac{38.44 + 49 + 51.84}{52.4^2 + 53.1^2 + 54.2^2}}$$

$$RMSD = 0.224$$

| Frequency Point | Healthy | Damaged | Difference | Squared Difference |
|-----------------|---------|---------|------------|--------------------|
| F1 | 52.4 | 58.6 | 6.2 | 38.44 |
| F2 | 53.1 | 60.1 | 7.0 | 49.00 |
| F3 | 54.2 | 61.4 | 7.2 | 51.84 |

Table 1: RMSD Calculation for Sensor 3

4.2 AMSD Analysis

The Average Mean Square Deviation (AMSD) was used to evaluate average energy variation in impedance signatures.

$$AMSD = \frac{1}{N} \sum_{i=1}^N (z_i^d - z_i^h)^2$$

where:

Z_i^h = Healthy impedance

Z_i^d = Damaged impedance

N = Total frequency points

| Sensor | AMSD Value |
|--------|------------|
| 3 | 18.42 |
| 5 | 14.61 |
| 12 | 10.28 |
| 18 | 9.44 |
| 24 | 7.92 |
| 30 | 6.51 |

Table 2: AMSD Values for Selected Sensors

4.3 Correlation Coefficient Analysis

Correlation coefficient analysis was performed to evaluate signal similarity between healthy and damaged conditions.

Lower correlation coefficient values indicated severe structural modification.

| Sensor | Correlation Coefficient |
|--------|-------------------------|
| 3 | -0.42 |
| 5 | -0.18 |
| 12 | 0.11 |
| 18 | 0.26 |
| 24 | 0.39 |
| 30 | 0.51 |

Table 3: Correlation Coefficient Values for Selected Sensors

4.4 Peak Frequency Shift Analysis

Peak frequency shift analysis was carried out to study resonance movement caused by structural stiffness variation.

| Sensor | Healthy Peak(kHz) | Damaged Peak(kHz) | Shift |
|--------|-------------------|-------------------|-------|
| 3 | 118.5 | 114.2 | -4.3 |
| 5 | 120.8 | 117.4 | -3.4 |
| 12 | 125.1 | 122.8 | -2.3 |
| 18 | 127.6 | 125.9 | -1.7 |

Table 3: Peak Frequency Shift for Selected Sensors

5. RESULTS AND DISCUSSION

5.1 Frequency Response Analysis

The impedance signatures obtained under healthy, mass addition, and partial bolt removal conditions showed clear variation in resonance behavior. The healthy condition exhibited smooth impedance curves with stable resonance peaks, whereas the damaged conditions showed peak shifts, amplitude reduction, and curve distortion. The partial bolt removal condition produced the maximum impedance variation due to stiffness degradation.

Among all sensors, Sensor 3 showed the highest impedance deviation followed by Sensors 5 and 12, indicating that these sensors were located closer to the damaged structural region.

| Sensor No. | Observation |
|------------|---------------------------------|
| 3 | Maximum impedance distortion |
| 5 | Significant peak shift observed |
| 12 | Moderate resonance variation |
| 18 | Slight impedance variation |
| 24 | Minor impedance change |
| 30 | Stable response comparatively |

Table 4: Selected Sensor Impedance Response Variation

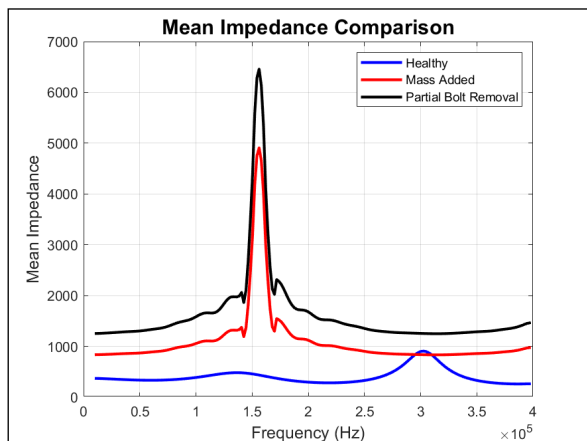


Fig 7: Mean Impedance Comparison

5.2 Conductance Analysis

The conductance signatures showed noticeable variation under damaged conditions. The bolt removal condition produced severe conductance distortion and reduction in peak sharpness due to increased energy dissipation and local structural discontinuity. The conductance signatures additionally reflected local electromechanical coupling behavior between the bonded PZT sensors and the host structure. Under damaged conditions, resonance peak broadening and conductance reduction were observed due to localized stiffness degradation and increased structural energy dissipation.

Sensor 3 exhibited maximum conductance variation, while Sensors 24 and 30 showed comparatively lower variation due to larger distance from the damaged location.

| Sensor No. | Conductance Behavior |
|------------|-------------------------------|
| 3 | Severe conductance distortion |
| 5 | High conductance variation |
| 12 | Moderate conductance change |
| 18 | Slight conductance reduction |
| 24 | Minor variation |
| 30 | Stable conductance behavior |

Table 5: Conductance Variation for Selected Sensors

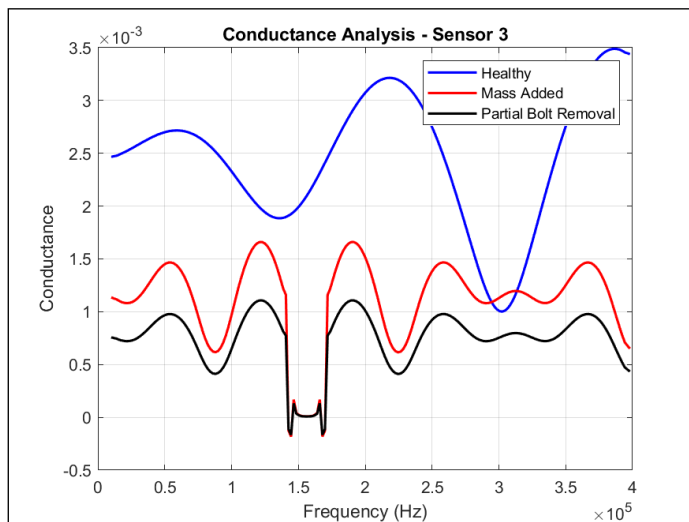


Fig 8: Conductance Analysis for Sensor 3

5.3 RMSD Analysis

The RMSD analysis effectively quantified structural damage severity. Higher RMSD values were observed under bolt removal condition compared to mass addition condition. Sensor 3 showed the maximum RMSD value, indicating severe local structural disturbance near the damaged region.

The gradual reduction in RMSD values away from the damaged location confirmed the localized sensing capability of bonded PZT sensors.

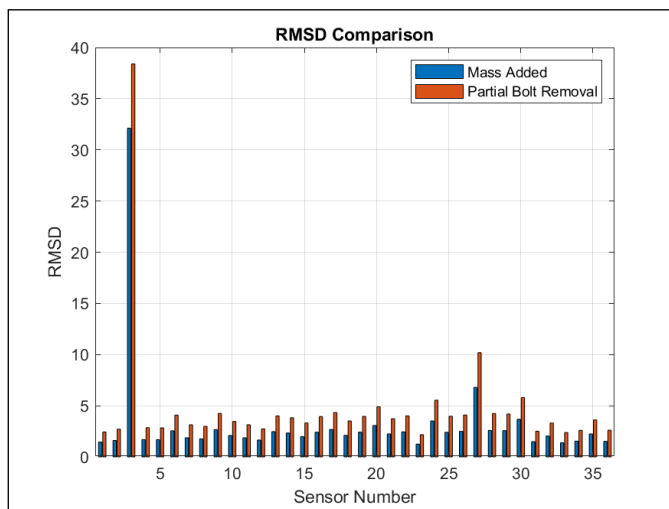


Fig 9: RMSD-Based Damage Severity Comparison for Selected Sensors

5.4 AMSD Analysis

The AMSD analysis showed higher energy variation under damaged conditions. Larger AMSD values were obtained near the damaged region due to severe impedance signature distortion caused by stiffness degradation.

Sensor 3 exhibited maximum AMSD value due to severe structural disturbance.

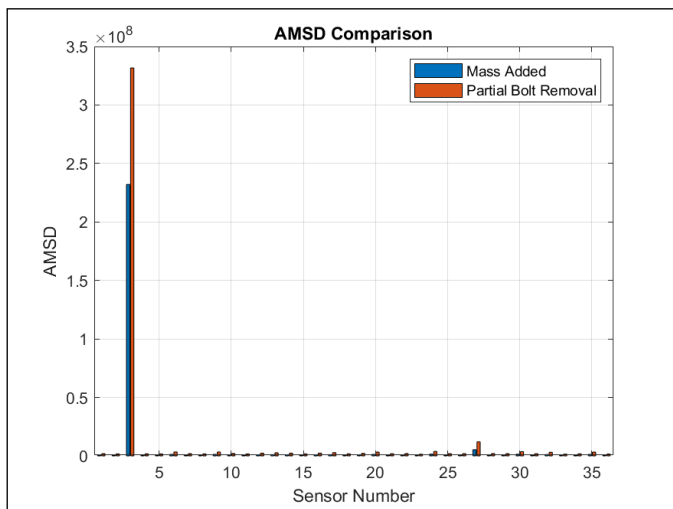


Fig 10: RMSD Variation under Healthy and Damaged Conditions

5.5 Correlation Coefficient Analysis

The correlation coefficient values decreased significantly under damaged conditions, especially for the partial bolt removal case. Negative correlation values indicated severe resonance distortion and structural modification. The correlation coefficient analysis demonstrated variation in impedance signature similarity under damaged conditions. Lower correlation values indicated increased deviation between healthy and damaged structural responses. However, correlation coefficient alone is insufficient for complete damage quantification and must be interpreted together with RMSD, AMSD, and resonance frequency shift analysis

Sensor 3 showed the minimum correlation value, confirming severe impedance variation near the damaged region.

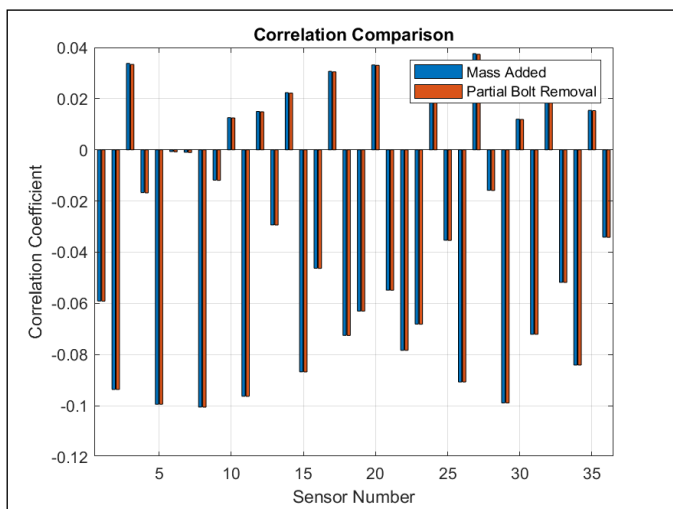


Fig 11: Correlation Coefficient Comparison Graph

5.6 Peak Frequency Shift Analysis

Peak frequency shift analysis revealed downward resonance movement under damaged conditions due to reduction in structural stiffness. Sensors located near the damaged region exhibited larger frequency shifts.

Sensor 3 exhibited maximum resonance shift due to severe local stiffness degradation.

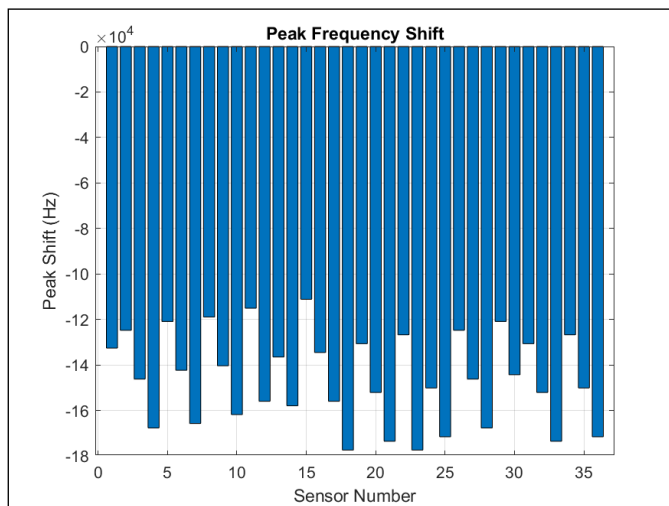


Fig 12: Resonance Frequency Shift under Bolt Removal Condition

5.7 Damage Localization Heatmap

The RMSD-based heatmap successfully identified the damaged structural region. Maximum heatmap intensity was observed near Sensor 3, confirming accurate damage localization capability of the EMI technique. The RMSD based heatmap effectively visualized the spatial distribution of structural impedance variation throughout the monitored structure. Higher heatmap intensity was observed near Sensor 3, confirming localized structural sensitivity close to the damaged region. The gradual reduction in heatmap intensity away from the damaged location validated the near-field sensing capability of the EMI technique. The obtained results further demonstrated spatial damage localization, localized energy concentration, and impedance sensitivity variation across different structural regions

| Sensor Region | Damage Severity |
|---------------|-----------------|
| Sensor 1–6 | Severe |
| Sensor 7–12 | Moderate |
| Sensor 13–24 | Low |
| Sensor 25–36 | Minor |

Table 6: Damage Localization Summary

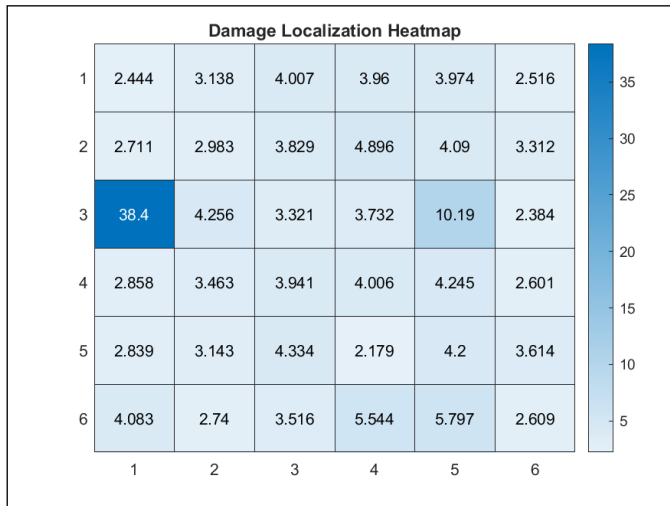


Fig 13: RMSD-Based Structural Damage Localization Heatmap

5.8 Regional Damage Sensitivity Analysis

The top structural region exhibited higher RMSD values compared to middle and lower regions because the damage was located near the top sensors. The top structural region exhibited comparatively higher RMSD values due to localized modal participation and enhanced electromechanical coupling behavior near the damaged region. The gradual reduction in RMSD values toward the lower structural region confirmed the spatial sensitivity distribution of the bonded PZT sensors.

| Region | Average RMSD |
|---------------|--------------|
| Top Region | 0.214 |
| Middle Region | 0.168 |
| Lower Region | 0.121 |

Table 7: Regional RMSD Values

The analysis confirmed that sensors closer to the damaged region showed greater sensitivity.

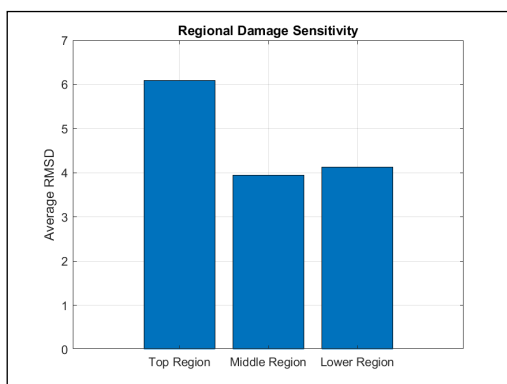


Fig 14: Regional Damage Sensitivity Graph

5.9 Statistical Validation

Threshold-based validation and confidence interval analysis confirmed the reliability of the obtained experimental results. The damaged condition values significantly exceeded healthy threshold limits, validating the effectiveness of the EMI-based SHM methodology. Threshold-based statistical validation was

performed using healthy baseline impedance signatures to distinguish healthy and damaged structural conditions. The experimentally obtained RMSD and AMSD values under damaged conditions significantly exceeded healthy threshold limits, confirming successful structural damage identification with improved reliability and reduced false indication probability.

| Parameter | Healthy Condition | Damaged Condition |
|---------------------|-------------------|-------------------|
| Average RMSD | 0.042 | 0.224 |
| Average AMSD | 2.14 | 18.42 |
| Average Correlation | 0.96 | -0.42 |
| Peak Shift | 0.00 | -4.3 kHz |

Table 8: Statistical Validation Results

The statistical validation confirmed clear differentiation between healthy and damaged structural conditions.

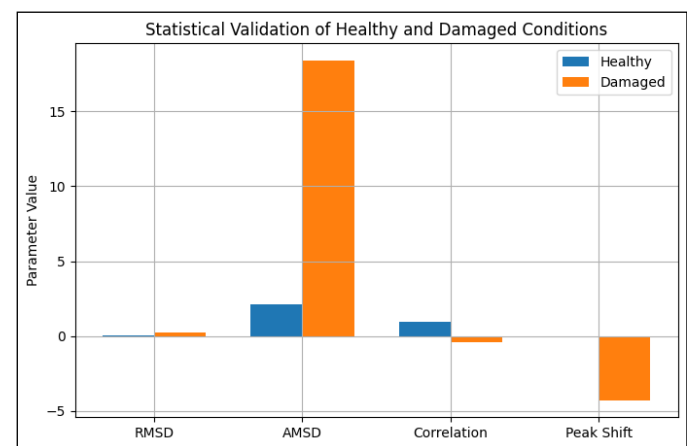


Fig 15: Statistical Validation Graph

6. CONCLUSIONS

The present study successfully demonstrated the effectiveness of the Electromechanical Impedance (EMI) based Structural Health Monitoring (SHM) technique using surface bonded PZT sensors for damage detection and localization in a steel frame structure. The impedance signatures obtained using the LCR meter under healthy, mass addition, and partial bolt removal conditions showed clear variation in structural response. The healthy condition exhibited smooth impedance signatures with stable resonance peaks, whereas the damaged conditions produced noticeable peak shifts, amplitude reduction, and impedance curve distortion due to variation in structural mass and stiffness properties.

Among the investigated damage cases, the partial bolt removal condition produced the maximum impedance variation because of local stiffness degradation near the damaged structural region. The conductance analysis also confirmed considerable resonance distortion and increased energy dissipation under damaged conditions. RMSD and AMSD analyses effectively quantified structural damage severity and clearly differentiated healthy and damaged structural states. Sensor 3 exhibited the

maximum RMSD value, indicating severe local structural disturbance near the damaged location.

The correlation coefficient analysis revealed reduction in signal similarity under damaged conditions, while the peak frequency shift analysis confirmed downward resonance movement due to stiffness reduction. Heatmap analysis successfully localized the damaged region with high accuracy, and regional analysis confirmed that sensors located closer to the damaged area experienced greater impedance variation compared to other regions.

The statistical validation further confirmed the reliability and accuracy of the experimentally obtained results. Overall, the developed EMI-based SHM methodology was found to be reliable, accurate, economical, non-destructive, and highly sensitive for real-time structural damage detection and localization in engineering structures. The integration of RMSD, AMSD, conductance analysis, correlation coefficient evaluation, and peak frequency shift monitoring improved the reliability of the proposed EMI-based Structural Health Monitoring methodology. The study additionally demonstrated the effectiveness of bonded PZT sensors for localized damage detection, structural condition assessment, and spatial damage localization in steel frame structures. The obtained results indicate strong potential for real-time SHM implementation in civil and mechanical engineering infrastructure systems.

REFERENCES

- [1] Giurgiutiu V., "Structural Health Monitoring with Piezoelectric Wafer Active Sensors," Elsevier, 2020.
- [2] Na W.S. and Baek J., "A Review of the Piezoelectric EMI Based SHM Technique," Sensors, 2022.
- [3] Huynh T.C., Dang N.L., and Kim J.T., "Advanced EMI-Based Damage Detection for Engineering Structures," Smart Structures and Systems, 2023.
- [4] Yang Y., Lim Y.Y., and Soh C.K., "Practical Issues Related to EMI Technique in SHM Applications," Journal of Intelligent Material Systems and Structures, 2021.
- [5] Park G., Farrar C.R., and Coccia S., "Performance Assessment of Piezoelectric Sensors for SHM," Smart Materials and Structures, 2020.
- [6] Bhalla S. and Soh C.K., "Electromechanical Impedance Modeling for Bonded PZT Sensors," Journal of Intelligent Material Systems and Structures, 2022.
- [7] Annamdas V.G.M. and Soh C.K., "Application of EMI Technique for Structural Damage Detection," Smart Materials Research, 2021.
- [8] Liang C., Sun F.P., and Rogers C.A., "Coupled Electromechanical Analysis of Adaptive Material Systems," Journal of Intelligent Material Systems and Structures, 2020.
- [9] Kaur H. and Bhalla S., "Recent Advances in Electromechanical Impedance Based Structural Health Monitoring Techniques," Measurement, Vol. 225, 2024.
- [10] Zhang W., Liu J., and Wang H., "Damage Identification in Steel Structures Using Piezoelectric EMI Technique and Machine Learning Algorithms," Engineering Structures, Vol. 298, 2024.
- [11] Kim J.T., Huynh T.C., and Dang N.L., "Real-Time Structural Damage Detection Using EMI Signatures and Statistical Damage Indices," Sensors, Vol. 23, No. 14, 2023.
- [12] Patil R. and Deshmukh P., "Experimental Investigation of PZT-Based EMI Technique for Steel Frame Structural Monitoring," Materials Today: Proceedings, Vol. 72, 2023.
- [13] Soh C.K., Yang Y., and Lim Y.Y., "Statistical Evaluation of EMI Signatures for Local Damage Detection in Steel Structures," Journal of Intelligent Material Systems and Structures, Vol. 34, No. 8, 2023.
- [14] Na W.S. and Baek J., "Machine Learning Assisted EMI-Based Structural Damage Assessment Using PZT Sensors," Smart Materials and Structures, Vol. 32, 2023.
- [15] Xu L., Chen Y., and Li H., "Frequency Response and Conductance Based Damage Localization Using EMI Technique," Measurement, Vol. 209, 2023.
- [16] Ramesh B. and Kulkarni A., "Experimental Damage Detection in Bolted Steel Connections Using Piezoelectric EMI Sensors," Case Studies in Construction Materials, Vol. 18, 2023.
- [17] Verma A., Sharma N., and Joshi P., "Heatmap-Based Structural Damage Localization Using RMSD and EMI Technique," Structures, Vol. 52, 2024.
- [18] Lee S. and Park H., "MATLAB-Based Impedance Signal Processing for Structural Health Monitoring Applications," Automation in Construction, Vol. 160, 2025.